PAPER

Heterogeneous diffusion with stochastic resetting

IOP Publishing Journal of Physics A: Mathematical and Theoretical
J. Phys. A: Math. Theor. **55** (2022) 074003 (26pp) https://doi.org/10.1088/1751-8121/ac491c

Heterogeneous diffusion with stochastic resetting

Trifce Sandev[1,2,3,*], Viktor Domazetoski[1], Ljupco Kocarev[1,4], Ralf Metzler[2] and Aleksei Chechkin[2,5,6]

[1] Research Center for Computer Science and Information Technologies, Macedonian Academy of Sciences and Arts, Bul. Krste Misirkov 2, 1000 Skopje, Macedonia
[2] Institute of Physics & Astronomy, University of Potsdam, D-14476 Potsdam-Golm, Germany
[3] Institute of Physics, Faculty of Natural Sciences and Mathematics, Ss. Cyril and Methodius University, Arhimedova 3, 1000 Skopje, Macedonia
[4] Faculty of Computer Science and Engineering, Ss. Cyril and Methodius University, PO Box 393, 1000 Skopje, Macedonia
[5] Faculty of Pure and Applied Mathematics, Hugo Steinhaus Center, Wroclaw University of Science and Technology, Wyspianskiego 27, 50-370 Wroclaw, Poland
[6] Akhiezer Institute for Theoretical Physics, Kharkov 61108, Ukraine

E-mail: trifce.sandev@manu.edu.mk

Received 10 November 2021, revised 28 December 2021
Accepted for publication 7 January 2022
Published 28 January 2022

Abstract

We study a heterogeneous diffusion process (HDP) with position-dependent diffusion coefficient and Poissonian stochastic resetting. We find exact results for the mean squared displacement and the probability density function. The nonequilibrium steady state reached in the long time limit is studied. We also analyse the transition to the non-equilibrium steady state by finding the large deviation function. We found that similarly to the case of the normal diffusion process where the diffusion length grows like $t^{1/2}$ while the length scale $\xi(t)$ of the inner core region of the nonequilibrium steady state grows linearly with time t, in the HDP with diffusion length increasing like $t^{p/2}$ the length scale $\xi(t)$ grows like t^{p}. The obtained results are verified by numerical solutions of the corresponding Langevin equation.

Keywords: heterogeneous diffusion, Fokker–Planck equation, Langevin equation, stochastic resetting, nonequilibrium stationary state, large deviation function

(Some figures may appear in colour only in the online journal)

*Author to whom any correspondence should be addressed.

1. Introduction

Anomalous diffusion is characterised by a mean squared displacement (MSD) of the power law form $\langle x^2(t)\rangle \sim t^{\beta}(\beta \neq 1)$ and has been observed in a wide variety of systems [1–5]. Consequently, it has been theoretically modelled in terms of different stochastic processes such as continuous time random walks with power-law distributed waiting times between successive jumps [6], as well as fractional Brownian motion [7] and the closely related fractional Langevin equation motion [8], which are driven by long-range correlated in time Gaussian noise. In general, these theoretical approaches are based on the assumption that the environment of the diffusing particle is homogeneous or that the heterogeneity of the media is coarse-grained over an increasing time or length scale, again leading to homogeneity.

However, various studies, including biological cells [9–11] and porous media [12, 13], have demonstrated that the underlying structure of the environment results in systematic variations of the local diffusion coefficient, and thus has a strong effect on the particle movement. These effects can be captured by heterogeneous diffusion models which describe the environment by using a position-dependent diffusion coefficient $\mathcal{D}(x)$ varying in space according to the power, exponential, or logarithmic laws [14]. Diffusion models with spatially varying diffusivity lead to anomalous diffusion and are used to describe transport processes on random fractals [15, 16], and in heterogeneous media [14, 17–25]. Heterogeneous diffusion processes (HDPs) in the following are defined as the motion of a diffusing particle subjected to a power-law space-dependent diffusion coefficient of form

$$\mathcal{D}(x) = \mathcal{D}_{\alpha}|x|^{\alpha}, \quad \alpha < 2. \tag{1}$$

The resulting MSD for HDPs behave as [14]

$$\langle x^2(t)\rangle \sim t^{p}, \quad p = \frac{2}{2-\alpha}, \tag{2}$$

which exhibits different diffusion regimes. Particularly, for $\alpha = 0$ ($p = 1$), we have normal diffusion. The case of subdiffusion is observed for $\alpha < 0$ ($0 < p < 1$), while superdiffusion for $0 < \alpha < 1$ ($1 < p < 2$). Additionally, for $1 < \alpha < 2$ ($p > 2$) one observes hyperdiffusion, and the result for $\alpha = 1$ corresponds to the ballistic motion ($p = 2$).

Motivated by optimal random search strategies, diffusion with stochastic resetting were introduced by Evans and Majumdar [26] who showed that the diffusing particles in presence of Poisson distributed reset to the initial position reach a non-equilibrium steady state (NESS) [26–29]. The mean first-passage time to a target [30] of a diffusive process in the presence of resetting, was shown to be reduced [26, 31–34]. The problem of stochastic resetting has been of interest in different contexts, starting from random search processes [30, 35–38], such as foraging dynamics [39] where the resetting can increase the performance of the search of foraging animals, for different diffusion processes [40–43], to quantum dynamics [44, 45]. Ergodicity in systems with resetting has also been recently analysed in references [46, 47]. An experimental realisation of the first-passage under stochastic resetting has been demonstrated in reference [48] with holographic optical tweezers. The number of papers on resetting in the last years is increasing so rapidly that it is impossible even to mention here all relevant directions of research. We refer to the recent review [28] for an exhaustive list of works in the field of stochastic resetting.

In this paper, we consider the problem of HDP with and without resetting. Analytical results for the probability density function (PDF) and MSD are found for the position-dependent diffusivity (1), including the transition dynamics to the stationary distribution. We show how the

obtained results turn to the known solution for a particular case when the initial position of a particle (and respectively, its position after the reset) coincides with the extremum of the diffusivity profile. We develop an alternative approach to analyse such a particular case in detail for a smooth diffusivity profile of form $\mathcal{D}(x) \sim (\epsilon + |x|)^{\alpha}$, $\epsilon > 0$, $\alpha < 2$.

The paper is organised as follows. In section 2 we analyse the heterogeneous diffusion without resetting and find the PDF and MSD. The corresponding heterogeneous diffusion model with resetting is introduced in section 3, where we find the PDF and corresponding MSD based on the results in absence of resetting. We also analyse their asymptotic behaviour. The transition dynamics to the NESS described by the large deviation function (LDF) is presented, as well. Specifically, in subsection 3.4 we simulate the HDP by using the Langevin equation with position-dependent diffusion coefficient and compare the results with our analytical theory. In section 4 we solve the heterogeneous diffusion equation with initial position at the origin $x_0 = 0$ and a smoothened diffusion coefficient of the form $\mathcal{D}(x) = (\epsilon + |x|)^{\alpha}$, $\epsilon > 0$ and $\alpha < 2$. Comparison between analytical results and simulations is quite favourable. A summary is provided in section 5. At the end of the paper in appendices A and B we provide details related to the calculation of the nth moment of the PDF, and to three equivalent representations of the HDP with stochastic resetting.

2. HDP without resetting

Let us consider an HDP obeying the Langevin equation with position-dependent diffusion coefficient

$$\dot{x}(t) = \sqrt{2\mathcal{D}(x)}\,\xi(t), \tag{3}$$

where $\xi(t)$ is white Gaussian noise with $\langle \xi(t) \rangle = 0$, $\langle \xi(t)\xi(t') \rangle = \delta(t - t')$. Equation (3) requires the choice of interpretation for the multiplicative noise, among which the Itô [49, 50], Stratonovich [51] and Hänggi–Klimontovich [52, 53] schemes are the most frequently used. The Stratonovich prescription is a natural choice if one aims to study the influence of an external noise with zero mean and short, but not infinitely short, autocorrelation time [54, 55]. In [56] the relevant reasons for using the Stratonovich interpretation for physical systems described by Langevin equations with non-additive fluctuations are discussed, particularly the consistency of the corresponding Fokker–Planck approach to the standard techniques used by physicists such as the cumulant expansion, projection operator and perturbative approaches. Such interpretation also seems most relevant for biological applications, since biological systems are typically far from equilibrium, the fluctuation–dissipation relation does not hold [57], and the Langevin equation approach with an external noise is meaningful [58]. Therefore, we here consider the HDP in the Stratonovich interpretation, while the corresponding problem in the Hänggi–Klimontovich and Itô interpretations will be analysed elsewhere [59]. With the position-dependent diffusivity (1), we here consider the Langevin equation [14, 24]

$$\dot{x}(t) = \sqrt{2\,\mathcal{D}_{\alpha}}\,|x|^{\alpha/2}\,\xi(t), \tag{4}$$

with corresponding Fokker–Planck equation for the PDF $P(x, t)$ [14, 24, 51]

$$\frac{\partial}{\partial t}P(x,t) = \mathcal{D}_{\alpha}\frac{\partial}{\partial x}\left\{|x|^{\alpha/2}\frac{\partial}{\partial x}\left[|x|^{\alpha/2}P(x,t)\right]\right\}. \tag{5}$$

The initial condition is given by $P(x,t=0)=\delta(x-x_0)$ while the boundary conditions are set to zero at infinity. We remind the readers that in the Stratonovich prescription stochastic integrals are treated in the same way as conventional integrals. Therefore, in order to analyse the HDP governed by equations (4) and (5), we introduce a new variable, see for example [14, 24],

$$y \equiv f(x) = p \times \mathrm{sgn}(x)\,|x|^{1/p}, \tag{6}$$

where $p=2/(2-\alpha)$ and $\mathrm{sgn}(x)$ is the sign function, which equals -1 for $x<0$, 0 for $x=0$, and 1 for $x>0$, such that $\mathrm{d}y/\mathrm{d}x = 1/|x|^{1-1/p}$. Therefore, by using $\dot{x}(t) = \frac{\mathrm{d}x}{\mathrm{d}t} = \frac{\mathrm{d}x}{\mathrm{d}y}\frac{\mathrm{d}y}{\mathrm{d}t} = |x|^{1-1/p}\dot{y}(t)$, equation (4) becomes a Langevin equation for ordinary Brownian motion, in $y(t)$,

$$\dot{y}(t) = \sqrt{2\,\mathcal{D}_\alpha}\,\xi(t). \tag{7}$$

Let us find the initial condition in respect to the variable y which corresponds to the initial condition $P(x,t=0)=\delta(x-x_0)$. By using the transformation

$$\bar{P}(y,t) = \int \delta(y-f(x))P(x,t)\,\mathrm{d}x \tag{8}$$

we find the new initial condition

$$\begin{aligned}\bar{P}(y,t=0) &= \int \delta(y-f(x))P(x,t=0)\,\mathrm{d}x \\ &= \int \delta\left(y - p\times\mathrm{sgn}(x)\,|x|^{1/p}\right)\delta(x-x_0)\,\mathrm{d}x = \delta(y-y_0),\end{aligned} \tag{9}$$

where $y_0 = p\times\mathrm{sgn}(x_0)|x_0|^{1/p}$. The solution of the diffusion equation, which corresponds to the Langevin equation (7), for initial condition $\bar{P}(y,t=0)=\delta(y-y_0)$ is the Gaussian PDF

$$\bar{P}(y,t) = \frac{1}{\sqrt{4\pi\mathcal{D}_\alpha t}}\,\exp\left(-\frac{[y-y_0]^2}{4\mathcal{D}_\alpha t}\right). \tag{10}$$

Knowing the PDF in respect to the variable y, we will find the PDF of the original problem, which is the solution of equation (5), through the transformation

$$P(x,t) = \int \delta\left(x - f^{-1}(y)\right)\bar{P}(y,t)\,\mathrm{d}y. \tag{11}$$

From relation (6), it follows that

$$x = \mathrm{sgn}(y)\frac{|y|^p}{p^p}, \tag{12}$$

and thus we have

$$P(x,t) = \frac{1}{\sqrt{4\pi\mathcal{D}_\alpha t}}\int \delta\left(x - \mathrm{sgn}(y)\frac{|y|^p}{p^p}\right)\exp\left(-\frac{[y-y_0]^2}{4\mathcal{D}_\alpha t}\right)\,\mathrm{d}y. \tag{13}$$

For the δ-function, we use the relation

$$\delta(g(y)) = \frac{\delta(y - y_i)}{\sum_i |g'(y_i)|}, \tag{14}$$

where y_i are the roots of $g(y)$, i.e. $g(y_i) = 0$. Here

$$g(y) = \mathrm{sgn}(y)\frac{|y|^p}{p^p} - x, \tag{15}$$

whose root is $y_i = p \times \mathrm{sgn}(x)|x|^{1/p}$, and

$$g'(y) = \frac{|y|^{p-1}}{p^{p-1}} \to |g'(y_i)| = |x|^{1-1/p} \tag{16}$$

and thus

$$\delta\left(\mathrm{sgn}(y)\frac{|y|^p}{p^p} - x\right) = \frac{\delta\left(y - p \times \mathrm{sgn}(x)|x|^{1/p}\right)}{|x|^{1-1/p}}. \tag{17}$$

Therefore, from equations (13) and (17), for the solution of the heterogeneous diffusion equation (5) one finds

$$P(x,t) = \frac{|x|^{1/p-1}}{\sqrt{4\pi\mathcal{D}_\alpha t}} \exp\left(-\frac{p^2\left[\mathrm{sgn}(x)\,|x|^{1/p} - \mathrm{sgn}(x_0)\,|x_0|^{1/p}\right]^2}{4\mathcal{D}_\alpha t}\right). \tag{18}$$

One can easily check that the PDF is normalised to one, see appendix A. For $x_0 = 0$, the PDF simplifies to [14]

$$P(x,t) = \frac{|x|^{1/p-1}}{\sqrt{4\pi\mathcal{D}_\alpha t}} \exp\left(-\frac{p^2|x|^{2/p}}{4\mathcal{D}_\alpha t}\right). \tag{19}$$

For $\alpha = 0$ ($p = 1$) the PDF yields the expected Gaussian form of the PDF. Notably, in the limit $\alpha = 2$, and $x, x_0 > 0$, the PDF (18) turns into the log-normal distribution for the geometric Brownian motion [23, 60, 61].

Let us now find the MSD $\langle x^2(t)\rangle = \int_{-\infty}^{\infty} x^2 P(x,t)\,\mathrm{d}x$. We obtain (see appendix A)

$$\langle x^2(t)\rangle = \frac{\Gamma(1+2p)}{p^{2p}}\frac{(\mathcal{D}_\alpha t)^p}{\Gamma(1+p)}\,{}_1F_1\left(-p, \frac{1}{2}, -p^2\frac{|x_0|^{2/p}}{4\mathcal{D}_\alpha t}\right), \tag{20}$$

where ${}_1F_1(a,b,z)$ is the confluent hypergeometric function of the first kind. For the limiting case $x_0 = 0$ (and thus ${}_1F_1(a,b,0) = 1$), we obtain the known result [14]

$$\langle x^2(t)\rangle = \frac{\Gamma(1+2p)}{p^{2p}}\frac{(\mathcal{D}_\alpha t)^p}{\Gamma(1+p)}. \tag{21}$$

For $\alpha = 0$ ($p = 1$) the MSD transforms to the MSD for Brownian motion $\langle x^2(t)\rangle = x_0^2 + 2\mathcal{D}_0 t$. By asymptotic expansion of (20) for $t \to \infty$, we have

$$\begin{aligned}\langle x^2(t)\rangle &\sim \frac{\Gamma(1+2p)}{p^{2p}}\frac{(\mathcal{D}_\alpha t)^p}{\Gamma(1+p)}\left[1 + 2p^3\frac{|x_0|^{2/p}}{4\mathcal{D}_\alpha t}\right] \\ &= C_1(p)(\mathcal{D}_\alpha t)^p + C_2|x_0|^{2/p}(\mathcal{D}_\alpha t)^{p-1},\end{aligned} \tag{22}$$

where $C_1(p) = \frac{\Gamma(1+2p)}{p^{2p}\Gamma(1+p)}$ and $C_2(p) = \frac{p^3}{2}C_1(p)$. Thus, for $t \to \infty$, the dominant term is $\langle x^2(t)\rangle \sim \frac{\Gamma(1+2p)}{p^{2p}} \frac{(\mathcal{D}_\alpha t)^p}{\Gamma(1+p)}$, which is the same as the MSD for $x_0 = 0$ as it shall be. For the case $\alpha = 0$ ($p = 1$) we recover the result for ordinary Brownian motion $\langle x^2(t)\rangle = 2\mathcal{D}_0 t + x_0^2$. For the short time limit $t \to 0$, the MSD behaves as $\langle x^2(t)\rangle \sim |x_0|^2 + 2(2p-1)|x_0|^{\frac{2(p-1)}{p}}\mathcal{D}_\alpha t$.

Results for the general-order moments, are given in appendix A. From these results one can analyse the kurtosis $k(t) = \frac{\langle (x-\langle x\rangle)^4\rangle}{(\langle x^2\rangle - \langle x\rangle^2)^2} - 3$ and skewness $g(t) = \frac{\langle (x-\langle x\rangle)^3\rangle}{(\langle x^2\rangle - \langle x\rangle^2)^{3/2}}$ of the obtained distribution.

3. HDP with resetting

We now study the situation when the particle motion governed by the heterogeneous diffusion equation (5) is interrupted after a random time interval τ by resetting the particle to its initial position. We consider a Poissonian resetting with the resetting time PDF $p(\tau) = r\,\mathrm{e}^{-r\tau}$. Therefore, the PDF $P_r(x,t|x_0)$ of the HDP with resetting can be expressed in terms of the PDF $P(x,t)$ of HDP in absence of resetting via the renewal equation [42, 62–64]

$$P_r(x,t|x_0) = \mathrm{e}^{-rt}P(x,t) + \int_0^t r\,\mathrm{e}^{-r\tau}P(x,\tau)\,d\tau, \tag{23}$$

meaning that each resetting event to the initial position x_0 renews the process at a rate r. Between two consecutive renewal events, the particle undergoes heterogeneous diffusion with position-dependent diffusion coefficient. The first term on the right-hand side of the equation corresponds to the case when there is no resetting event up to time t, while the second term describes multiple resetting events.

3.1. Probability density function of the HDP with resetting

By taking the Laplace transform of equation (23), one concludes that the PDF of the process with resetting can be calculated from the PDF in absence of resetting in Laplace space via

$$\hat{P}_r(x,s|x_0) = \frac{s+r}{s}\hat{P}(x,s+r), \tag{24}$$

where $\hat{P}(x,s)$ is the Laplace transform of the PDF (18),

$$\hat{P}(x,s) = \mathscr{L}[P(x,t)] = \frac{|x|^{1/p-1}}{\sqrt{4\mathcal{D}_\alpha}}s^{-1/2}\ \exp\left(-p\left|\mathrm{sgn}(x)|x|^{1/p} - \mathrm{sgn}(x_0)|x_0|^{1/p}\right|\sqrt{\frac{s}{\mathcal{D}_\alpha}}\right). \tag{25}$$

In the long time limit, we find that the PDF reaches the NESS given by

$$\begin{aligned} P_{r,\mathrm{st}}(x) &= \lim_{t\to\infty} P_r(x,t|x_0) = \lim_{s\to 0} s\hat{P}_r(x,s|x_0) = r\hat{P}(x,r) \\ &= \frac{|x|^{1/p-1}}{\sqrt{4\mathcal{D}_\alpha/r}}\exp\left(-p\frac{\left|\mathrm{sgn}(x)|x|^{1/p} - \mathrm{sgn}(x_0)|x_0|^{1/p}\right|}{\sqrt{\mathcal{D}_\alpha/r}}\right). \end{aligned} \tag{26}$$

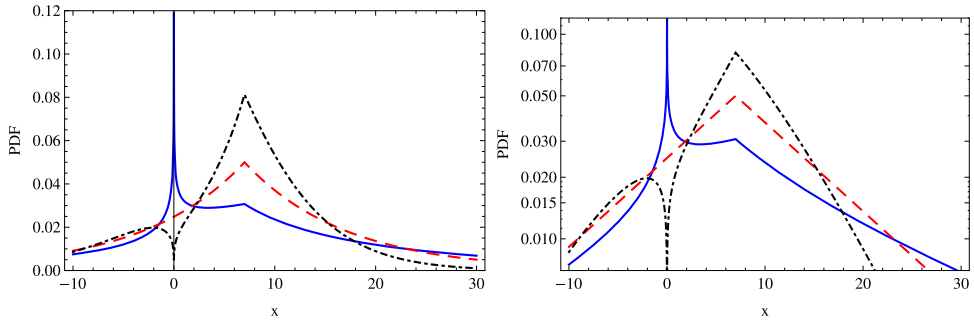

Figure 1. Graphical representation of the PDF (23) in the NESS, equation (26), for $\mathcal{D}_\alpha = 1$, $x_0 = 7$, $r = 0.01$ and $\alpha = 0.5$ (blue solid line), $\alpha = 0$ (the Laplace distribution, red dashed line), $\alpha = -0.5$ (black dotted line). Linear–linear plot in the left panel and log–linear plot in the right panel.

For $x_0 = 0$, the PDF in the NESS reads

$$P_{r,\mathrm{st}}(x) = \frac{|x|^{1/p-1}}{\sqrt{4\mathcal{D}_\alpha/r}} \exp\left(-p\frac{|x|^{1/p}}{\sqrt{\mathcal{D}_\alpha/r}}\right), \tag{27}$$

which was obtained in reference [47]. For $\alpha = 0$, equation (26) reduces to the PDF in the NESS for the normal diffusion process with stochastic resetting [26]

$$P_{\mathrm{st}}(x) = \frac{1}{\sqrt{4\pi\mathcal{D}_0/r}} \exp\left(-\frac{|x-x_0|}{\sqrt{\mathcal{D}_0/r}}\right). \tag{28}$$

A graphical representation of the PDF in the NESS (26) is shown in figure 1. From the figure we observe that for $\alpha = 1/2$ the PDF has a sharp maximum at $x = 0$, while for $\alpha = -1/2$ it has a minimum. These extrema can be explained qualitatively as follows. For small x and $\alpha > 0$ the intensity of the multiplicative noise in the Langevin equation becomes very small, and thus the particle spends more time around the origin before it resets to the initial position x_0. On the contrary, for small x and $\alpha < 0$ the intensity of the multiplicative noise becomes very large, and the particle does not spend much time near the origin. Also, the cusp of the PDF in the initial position x_0 to which the particle is reset is observed since the resetting mechanism introduces a source of probability at x_0.

3.2. Mean squared displacement of the HDP with resetting

After multiplication of both sides of equation (24) by x^2 and integration over x, we find the MSD in Laplace space,

$$\left\langle \hat{x}^2(s)\right\rangle_r = \int_{-\infty}^{\infty} x^2\, \hat{P}_r(x,s|x_0)\,\mathrm{d}x = \frac{s+r}{s}\left\langle \hat{x}^2(s+r)\right\rangle, \tag{29}$$

where $\left\langle \hat{x}^2(s)\right\rangle$ is the Laplace transform of equation (20). The inverse Laplace transform of equation (29) yields

$$\left\langle x^2(t)\right\rangle_r = \mathrm{e}^{-rt}\left\langle x^2(t)\right\rangle + \int_0^t r\,\mathrm{e}^{-rt'}\left\langle x^2(t')\right\rangle\,\mathrm{d}t', \tag{30}$$

where $\langle x^2(t)\rangle$ is given by equation (20). From here we find the long time behaviour of the MSD in presence of resetting, which reads

$$\langle x^2(t)\rangle_r \sim \int_0^\infty r\,\mathrm{e}^{-rt'}\,\langle x^2(t')\rangle\,\mathrm{d}t' = r\,\langle \hat{x}^2(s=r)\rangle\,, \tag{31}$$

where $\langle \hat{x}^2(s)\rangle$ is the Laplace transform of the MSD (20) calculated at $s = r$. The short time limit yields the same behaviour of the MSD as in the case without resetting, see equation (20).

For $x_0 = 0$, from equations (21) and (29), for the MSD we find the general form

$$\langle x^2(t)\rangle = \frac{\Gamma(1+2p)}{p^{2p}}\mathcal{D}_\alpha^p\mathcal{L}^{-1}\left[\frac{s^{-1}}{(s+r)^p}\right] = \frac{\Gamma(1+2p)}{p^{2p}}\mathcal{D}_\alpha^p t^p E_{1,p+1}^p(-rt), \tag{32}$$

where

$$E_{\rho,\beta}^\delta(z) = \sum_{n=0}^\infty \frac{(\delta)_n}{\Gamma(\rho n+\beta)}\frac{z^n}{n!} \tag{33}$$

is the three parameter Mittag–Leffler function [65], with the Pochhammer symbol $(\delta)_n = \Gamma(\delta+n)/\Gamma(\delta)$. By asymptotic expansion of the three parameter Mittag–Leffler function [66]

$$E_{\rho,\beta}^\delta(-z) = \frac{z^{-\delta}}{\Gamma(\delta)}\sum_{n=0}^\infty \frac{\Gamma(\delta+n)}{\Gamma(\beta-\rho(\delta+n))}\frac{(-z)^{-n}}{n!}, \tag{34}$$

with $z > 1$, and $0 < \rho < 2$, for the MSD in the short and long time limit we find

$$\langle x^2(t)\rangle \sim \frac{\Gamma(1+2p)}{p^{2p}}\mathcal{D}_\alpha^p\begin{cases} t^p/\Gamma(1+p)\,, & rt \ll 1,\\ 1/r^p, & rt \gg 1.\end{cases} \tag{35}$$

In the long time limit, the MSD tends to a constant, thus indicating the emergence of a NESS.

3.3. Transition to the stationary state

From equations (27) and (35) we see that the system reaches a NESS. This also can be shown from the renewal equation (23) as the dominant contribution in the long time limit comes from the second (integral) term of the equation.

The analysis of the transition to the steady state might be far from a trivial task. In a system with $x \to -x$ symmetry, the NESS is established in an inner core region $[-\xi(t), \xi(t)]$ around the point x_0 to which the system is reset, where $\xi(t)$ is the time-dependent length scale. Outside of this region, the system is in a transient state, which is not yet relaxed to the NESS. In absence of an $x \to -x$ symmetry, the NESS is established in an inner core region $[-\xi_-(t), \xi_+(t)]$ around the point to which the system is reset. This region grows as $\xi_\pm(t) \sim t^{1/\varepsilon_\pm}$ [28, 67, 68], where $\epsilon_\pm$ are positive exponents, which depend on the particular underlying displacement process[7]. On this scale $x \sim \xi_\pm(t)$ the PDF has the large deviation form

$$P_r(x,t|x_0) \sim \exp\left(-t\,I(x/\xi_\pm(t))\right), \tag{36}$$

[7] For example, for the normal diffusion process without resetting, the typical diffusion length scale grows algebraically as $t^{1/2}$, i.e. $\epsilon = 2$, while in case of Poissonian resetting it grows as t^1, i.e. $\epsilon = 1$ [26, 28].

where $I(w)$ is the LDF [67].

Let us estimate the integral term in the renewal equation (23) by the Laplace method [28, 67]. By using $t' = t\tau$, i.e. $\mathrm{d}t' = t\,\mathrm{d}\tau$, we have

$$r\int_0^t \mathrm{e}^{-rt'}\,P(x,t')\,\mathrm{d}t' = \frac{r|x|^{1/p-1}}{\sqrt{4\pi\mathcal{D}_\alpha}}\int_0^\infty \frac{\exp\left(-rt' - \frac{p^2\left[\mathrm{sgn}(x)\,|x|^{1/p}-\mathrm{sgn}(x_0)\,|x_0|^{1/p}\right]^2}{4\mathcal{D}_\alpha t'}\right)\mathrm{d}t'}{\sqrt{t'}}$$
$$= \frac{r|x|^{1/p-1}}{\sqrt{4\pi\mathcal{D}_\alpha}}\sqrt{t}\int_0^1 \tau^{-1/2}\,\mathrm{e}^{-t\Phi(\tau,w)}\,\mathrm{d}\tau, \tag{37}$$

where

$$\Phi(\tau,w) = r\tau + p^2\frac{w^2}{4\mathcal{D}_\alpha\tau}, \tag{38}$$

and

$$w = \frac{\left|\mathrm{sgn}(x)|x|^{1/p} - \mathrm{sgn}(x_0)\,|x_0|^{1/p}\right|}{t}.$$

From here, one concludes that if $\mathrm{sgn}(x) = \mathrm{sgn}(x_0)$ we have $w_\mathrm{e} = \left||x|^{1/p} - |x_0|^{1/p}\right|/t$, while if $\mathrm{sgn}(x) \neq \mathrm{sgn}(x_0)$ we have $w_\mathrm{ne} = \left(|x|^{1/p} + |x_0|^{1/p}\right)/t$. Next, we should estimate the integral of the form

$$\mathcal{I}(t) = \int_0^1 \mathrm{e}^{-tf(z)}\,g(z)\mathrm{d}z \tag{39}$$

for large t. With the Laplace method it is given by [69]

$$\mathcal{I}(t) \approx \mathrm{e}^{-tf(z_0)}\,g(z_0)\sqrt{\frac{2\pi}{t|f''(z_0)|}}, \tag{40}$$

which requires the evaluation of the minimum of the function $f(z)$, i.e. $f'(z_0) = 0$, if $0 < z_0 < 1$. If the extremum point z_0 is outside the integration limits ($z_0 > 1$), then the approximation result is calculated at $z_0 = 1$. In our case, the function $f(z)$ corresponds to the function $\Phi(\tau,w)$, with $z \to \tau$. Thus, from $\frac{\mathrm{d}}{\mathrm{d}\tau}\Phi(\tau,w)\big|_{\tau=\tau_*} = 0$ we find

$$\tau_* = \frac{p}{\sqrt{4\mathcal{D}_\alpha r}}w \tag{41}$$

and one can see that the PDF in the NESS has the form of equation (36), where $\xi(t) \sim t^p$, and the LDF is given by

$$I(w) = \begin{cases} p\sqrt{\dfrac{r}{\mathcal{D}_\alpha}}w, & \left|\mathrm{sgn}(x)|x|^{1/p} - \mathrm{sgn}(x_0)|x_0|^{1/p}\right| \leqslant \dfrac{(4\mathcal{D}_\alpha r)^{1/2}}{p}t, \\ r + \dfrac{p^2}{4\mathcal{D}_\alpha}w^2, & \left|\mathrm{sgn}(x)|x|^{1/p} - \mathrm{sgn}(x_0)|x_0|^{1/p}\right| \geqslant \dfrac{(4\mathcal{D}_\alpha r)^{1/2}}{p}t. \end{cases} \tag{42}$$

Therefore, for $\mathrm{sgn}(x) = \mathrm{sgn}(x_0)$, the LDF reads

$$I(w_{\mathrm{e}}) = \begin{cases} p\sqrt{\dfrac{r}{\mathcal{D}_\alpha}}w_{\mathrm{e}}, & \left||x|^{1/p} - |x_0|^{1/p}\right| \leqslant \dfrac{(4\mathcal{D}_\alpha r)^{1/2}}{p}t, \\ r + \dfrac{p^2}{4\mathcal{D}_\alpha}w_{\mathrm{e}}^2, & \left||x|^{1/p} - |x_0|^{1/p}\right| \geqslant \dfrac{(4\mathcal{D}_\alpha r)^{1/2}}{p}t, \end{cases} \tag{43}$$

and

$$I(w_{\mathrm{ne}}) = \begin{cases} p\sqrt{\dfrac{r}{\mathcal{D}_\alpha}}w_{\mathrm{ne}}, & |x|^{1/p} + |x_0|^{1/p} \leqslant \dfrac{(4\mathcal{D}_\alpha r)^{1/2}}{p}t, \\ r + \dfrac{p^2}{4\mathcal{D}_\alpha}w_{\mathrm{ne}}^2, & |x|^{1/p} + |x_0|^{1/p} \geqslant \dfrac{(4\mathcal{D}_\alpha r)^{1/2}}{p}t, \end{cases} \tag{44}$$

for $\mathrm{sgn}(x) \neq \mathrm{sgn}(x_0)$.

For the symmetric case $x_0 = 0$, we find

$$\Phi(\tau, w) = r\tau + \frac{p^2}{4\mathcal{D}\tau}w^{2/p}, \tag{45}$$

and

$$I\left(\frac{|x|}{\xi(t)}\right) = \begin{cases} p\sqrt{\dfrac{r}{\mathcal{D}}}\left(\dfrac{|x|}{t^p}\right)^{1/p}, & |x| \leqslant (4p^2\mathcal{D}_\alpha r)^{p/2}t^p, \\ r + \dfrac{p^2}{4\mathcal{D}_\alpha}\left(\dfrac{|x|}{t^p}\right)^{2/p}, & |x| \geqslant (4p^2\mathcal{D}_\alpha r)^{p/2}t^p. \end{cases} \tag{46}$$

It generalises the classical result for normal Brownian motion to the case of anomalous diffusion. Indeed, in normal diffusion, the diffusion length grows like $t^{1/2}$, whereas the length scale $\xi(t)$ grows linearly with t. In anomalous diffusion, we have the diffusion length $\sim t^{p/2}$, whereas $\xi(t)$ grows like t^p. So, this anomalous scaling is fully consistent with the normal diffusion behaviour under the reset. We also conclude that the boundary between the NESS region and the transient region given in equation (46) moves with a non-constant velocity given by

$$v(t) = p\left(4p^2\mathcal{D}_\alpha r\right)^{p/2}t^{p-1} \simeq t^{\alpha/(2-\alpha)}. \tag{47}$$

In the case of a constant diffusion coefficient ($\alpha = 0$), we recover the constant velocity of the boundary between the region with NESS and the transient region, given by $v = \sqrt{4\mathcal{D}_0 r}$ [28, 67].

The LDF (46) for different α is shown in figure 2. All trajectories that satisfy $|x| \leqslant (4p^2\mathcal{D}_\alpha r)^{p/2}\, t^p$ relax to the NESS, represented by the first line in the LDF (46). Those trajectories have experienced a large number of resetting events. The trajectories for which $|x| \geqslant (4p^2\mathcal{D}_\alpha r)^{p/2}\, t^p$ (second line of equation (46)) are in the transient regime. Those particles have experienced almost no resetting up to time t, which is a very rare event, and the corresponding probability density is of the form $\mathrm{e}^{-rt}P(x,t)$, where $P(x,t)$ is the PDF of the process without resetting. In figure 3 we represent the PDF (23) for different parameters α at $t = 100$. For plotting the PDF we use relations (24) and (25) for $x_0 = 0$, and employ the numerical inverse Laplace transform algorithm in Mathematica [70].

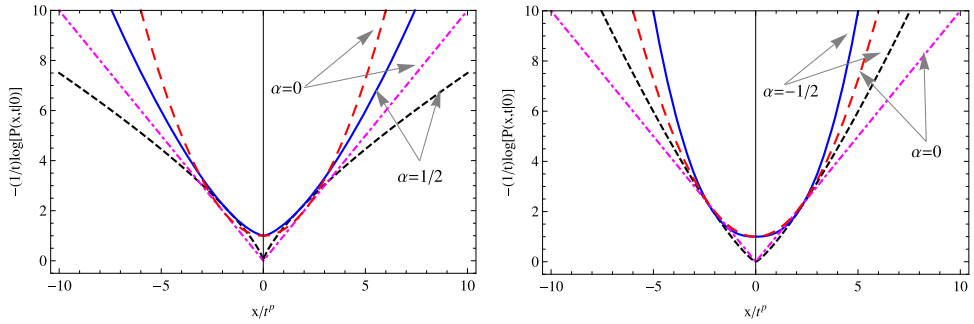

Figure 2. LDF (46) for $\mathcal{D}_\alpha = 1$, $r = 1$ plotted in scaled form. Black dotted line and blue solid line correspond to the first and second lines in equation (46), respectively, for $\alpha = 0.5$ in the left panel and $\alpha = -0.5$ in the right panel. Pink dot–dashed line and red dashed line correspond to the first and second lines in equation (46), respectively, for $\alpha = 0$.

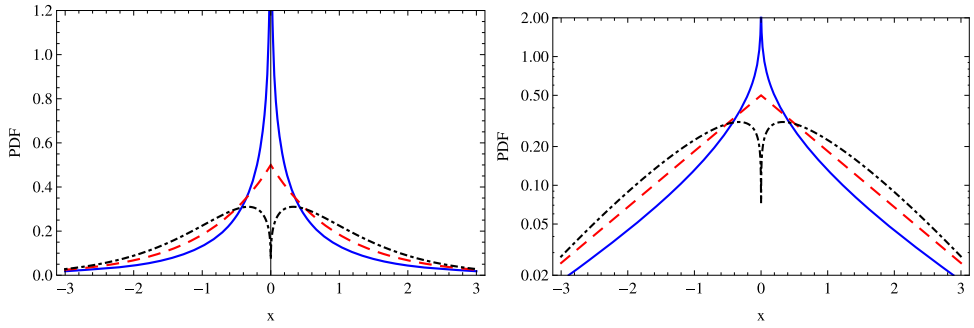

Figure 3. PDF for $\mathcal{D}_\alpha = 1$, $r = 1$ and $x_0 = 0$ and $t = 100$ for $\alpha = 0.5$ (blue solid line), $\alpha = 0$ (red dashed line) and $\alpha = -0.5$ (black dot–dashed line). Linear–linear plot in the left panel and log–linear plot in the right panel.

3.4. Numerical simulations

In order to perform numerical simulations of the HDP with stochastic resetting, we consider the Langevin equation in the presence of resetting (see references [71, 72])

$$x(t+\Delta t) = \begin{cases} x(0), & \text{with prob. } r\Delta t, \\ x(t) + \sqrt{2\mathcal{D}(x)\Delta t}\,\eta(t) + \dfrac{2-A}{2}\sqrt{2\,\mathcal{D}(x)}\dfrac{\mathrm{d}\sqrt{2\mathcal{D}(x)}}{\mathrm{d}x}\Delta t, & \text{with prob. } (1-r\Delta t). \end{cases} \tag{48}$$

Here we introduce an additional positive parameter A which allows one to consider different interpretations of the Langevin equation. Namely, at $A = 1$ we get a discretised version of the Langevin equation in Stratonovich interpretation, which we use in our analytical calculations. The drift term in equation (48) is a consequence of the conversion of the Stratonovich stochastic differential equation equation (3) into an Itô stochastic differential equation which is then integrated using the Euler–Maruyama scheme (see [24, 73, 74]). The equation corresponds to the

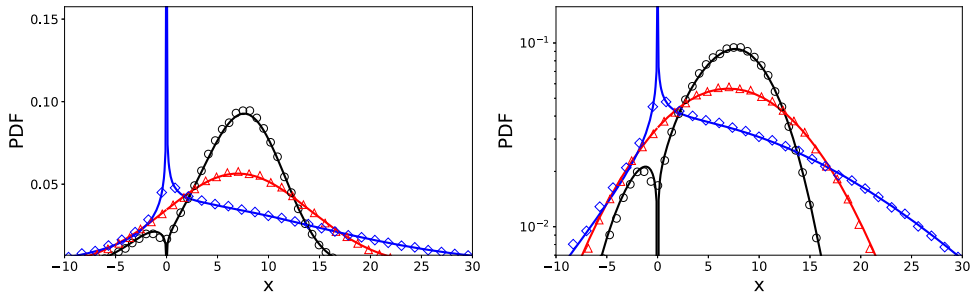

Figure 4. PDF (18) in the absence of resetting for $\mathcal{D}_\alpha = 1$, $x_0 = 7$, $t = 25$, $r = 0$ and $\alpha = 0.5$ (blue line), $\alpha = 0$ (red line), and $\alpha = -0.5$ (black line). Results from Langevin simulations are shown by squares, triangles and circles for $\alpha = 0.5, 0$ and -0.5, respectively. The PDF shapes are shown in linear (left panel) and log–linear (right panel) scales.

Itô interpretation for $A = 2$ and can be also used to model the Klimontovich–Hänggi interpretation when using $A = 0$. In order to avoid particle trapping and divergencies of the diffusion coefficient at the origin $x = 0$, we use a modified form of the diffusion coefficient such that $\mathcal{D}(x) = \mathcal{D}_\alpha(\epsilon + |x|)^\alpha$. All simulations have been performed with $\epsilon = 0.1$ and $\Delta t = 0.01$. The noise $\eta(t)$ is sampled from the Gaussian normal distribution $N(0, \Delta t)$. The effect of stochastic resetting is modelled by sampling a resetting time from an exponential distribution with a rate r, representing the time between two events in a Poisson point process. In between two events the particle undergoes heterogeneous diffusion and resets at x_0 afterwards. To analyse the temporal evolution of the PDF, we simulate an ensemble of 1.5×10^6 particles for different values of α (such that $\alpha < 2$) across a time span of 10^4 to observe the convergence of the process to the stationary state.

Graphical representations of the PDF for different values of α are shown in figure 4 for the case without resetting and in figure 5 for the case with resetting. For plotting the analytical results for the PDF we use the numerical inverse Laplace transform algorithm in Mathematica [70]. Excellent agreement with the simulations is observed. The MSD obtained from the analytical results and the simulations is presented in figure 6. From the figure, one observes that the MSD saturates at around $t = 10^3$. This means that the PDF reaches the NESS at times beyond $t = 10^3$. In figure 7 we plot the PDF at $t = 1000$ and we observe that it coincides with the PDF (23) in the NESS.

4. HDP with smooth diffusivity profile

The HDP with resetting to the initial position $x_0 = 0$ can be represented by the following equation

$$\frac{\partial}{\partial t}P_r(x,t|0) = \frac{\partial}{\partial x}\left\{\sqrt{\mathcal{D}(x)}\frac{\partial}{\partial x}\left[\sqrt{\mathcal{D}(x)}P_r(x,t|0)\right]\right\} - rP_r(x,t|0) + r\delta(x), \tag{49}$$

with $P_r(x, t = 0|0) = \delta(x)$, and position-dependent diffusion coefficient of the form $\mathcal{D}(x) = \mathcal{D}_\alpha(\epsilon + |x|)^\alpha$, and where r is the rate of resetting to the initial position $x_0 = 0$. The second term on the right-hand side of equation (49) represents the loss of probability from the position x due to reset to the initial position $x_0 = 0$, and the third term accounts for the gain of probability at $x_0 = 0$ due to resetting from all other positions. For $\alpha = 0$ one obtains the standard diffusion

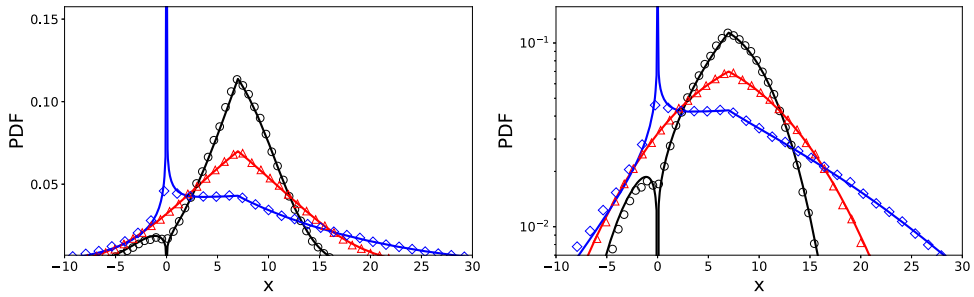

Figure 5. PDF (23) in the presence of resetting for $\mathcal{D}_\alpha = 1, x_0 = 7, t = 25, r = 0.01$ and $\alpha = 0.5$ (blue line), $\alpha = 0$ (red line), and $\alpha = -0.5$ (black line). Langevin simulations results are shown by squares, triangles and circles for $\alpha = 0.5, 0$ and -0.5, respectively. The PDF shapes are shown in linear (left panel) and log–linear (right panel) scales.

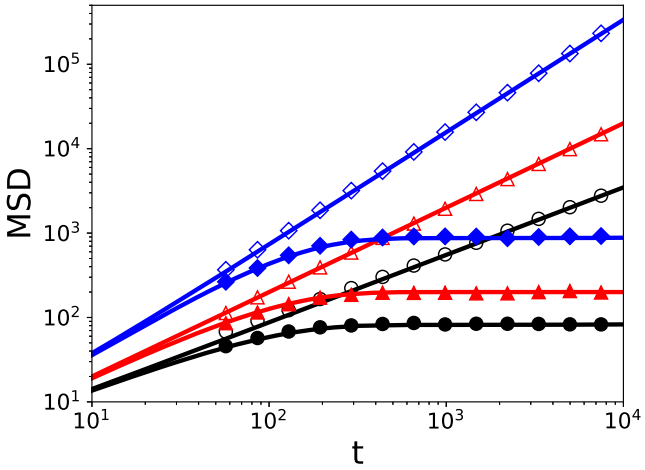

Figure 6. MSD in the absence ($r = 0$) and presence of resetting ($r = 0.01$) for $\mathcal{D}_\alpha = 1$, $x_0 = 1$ and $\alpha = 0.5$ (blue lines), $\alpha = 0$ (red lines), $\alpha = -0.5$ (black lines). Langevin simulations results for $\alpha = 0.5$ are shown by white squares ($r = 0$) and blue squares ($r = 0.01$), for $\alpha = 0$ by white triangles ($r = 0$) and red triangles ($r = 0.01$), and for $\alpha = -0.5$ by white circles ($r = 0$) and black circles ($r = 0.01$).

equation with stochastic resetting [26, 27, 41]. In what follows, we solve equation (49) and show the connection with the results obtained above. For alternative representations of HDP with stochastic resetting see appendix B.

4.1. PDF

The Laplace transform of equation (49) reads

$$(s+r)\hat{P}_r(x,s|0) - s^{-1}(s+r)\delta(x) = \mathcal{D}_\alpha \frac{\partial}{\partial x}\left\{(\epsilon+|x|)^{\alpha/2} \times \frac{\partial}{\partial x}\left[(\epsilon+|x|)^{\alpha/2}\hat{P}_r(x,s|0)\right]\right\}. \quad (50)$$

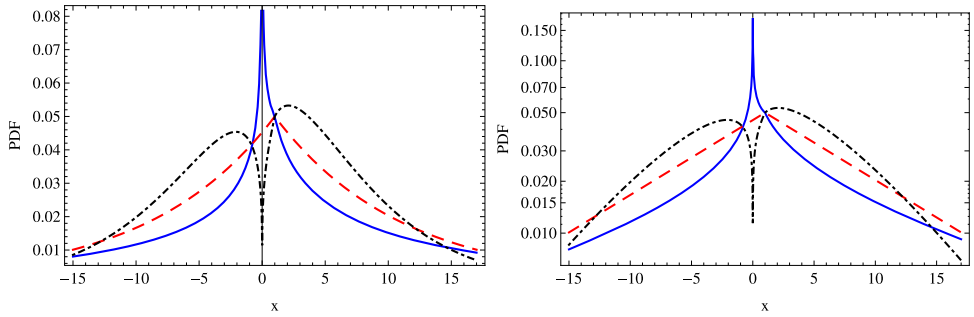

Figure 7. PDF (23) in the presence of resetting for $\mathcal{D}_\alpha = 1$, $x_0 = 1$, $t = 1000$, $r = 0.01$ and $\alpha = 0.5$ (blue solid line), $\alpha = 0$ (red dashed line), and $\alpha = -0.5$ (black dot–dashed line). The PDF shapes are shown in linear (left panel) and log–linear (right panel) scales. We checked that the PDF at $t = 10^3$ coincides with the PDF (23) in the NESS, equation (26).

By differentiation with respect to x one finds

$$(s+r)\hat{P}_r(x,s|0) - s^{-1}(s+r)\delta(x) = \mathcal{D}_\alpha \Big[\alpha\delta(x)(\epsilon+|x|)^{\alpha-1}\hat{P}_r(x,s|0) + \frac{(\alpha-1)\alpha}{2}(\epsilon+|x|)^{\alpha-2}\hat{P}_r(x,s|0) + (2\theta(x)-1)\frac{3\alpha}{2}(\epsilon+|x|)^{\alpha-1}\frac{\partial}{\partial x}\hat{P}_r \times (x,s|0) + (\epsilon+|x|)^{\alpha}\frac{\partial^2}{\partial x^2}\hat{P}_r(x,s|0)\Big], \tag{51}$$

where $\theta(x)$ is the Heaviside step function. By using $|x| = y$, $\hat{P}_r(|x|,s|0) = \hat{P}_r(y,s|0) = \mathcal{C}_\epsilon(s)\hat{f}(y,s|0)$ and $\frac{\mathrm{d}}{\mathrm{d}x}\theta(x) = \delta(x)$, we transform equation (51) to

$$(s+r)\mathcal{C}_\epsilon(s)\hat{f}(y,s|0) - s^{-1}(s+r)\delta(x) = \mathcal{D}_\alpha\frac{(\alpha-1)\alpha}{2}\mathcal{C}_\epsilon(s)(\epsilon+y)^{\alpha-2}\hat{f}(y,s|0) + \mathcal{D}_\alpha\,\alpha(\epsilon+y)^{\alpha-1}\mathcal{C}_\epsilon(s)\delta(x)\hat{f}(y,s|0) + \mathcal{D}_\alpha\frac{3\alpha}{2}(\epsilon+y)^{\alpha-1}\mathcal{C}_\epsilon(s)\frac{\partial}{\partial y}\hat{f}(y,s|0) + 2\mathcal{D}_\alpha\mathcal{C}_\epsilon(s)(\epsilon+y)^{\alpha}\delta(x)\frac{\partial}{\partial y}\hat{f}(y,s|0) + \mathcal{D}_\alpha\mathcal{C}_\epsilon(s)(\epsilon+y)^{\alpha}\frac{\partial^2}{\partial y^2}\hat{f}(y,s|0). \tag{52}$$

Therefore, we obtain the system of equations

$$\begin{cases} \dfrac{\partial^2}{\partial y^2}\hat{f}(y,s|0) + \dfrac{3\alpha/2}{\epsilon+y}\dfrac{\partial}{\partial y}\hat{f}(y,s|0) + \left[-\dfrac{(s+r)}{\mathcal{D}_\alpha}(\epsilon+y)^{-\alpha} + \dfrac{(\alpha-1)\alpha}{2}\dfrac{1}{(\epsilon+y)^2}\right]\hat{f}(y,s|0) = 0, \\ -s^{-1}(s+r) = \mathcal{D}_\alpha\,\mathcal{C}_\epsilon(s)\left[\alpha(\epsilon+y)^{\alpha-1}\hat{f}(y,s|0) + 2(\epsilon+y)^{\alpha}\dfrac{\partial}{\partial y}\hat{f}(y,s|0)\right]\Big|_{y=0}. \end{cases} \tag{53}$$

The first equation in (53) is the Lommel-type equation [75] ($\epsilon + y \to \bar{y}$)

$$z''(\bar{y}) + \frac{1-2\beta'}{\bar{y}} z'(\bar{y}) + \left[\left(a\alpha' \bar{y}^{\alpha'-1} \right)^2 + \frac{\beta'^2 - \nu^2 \alpha'^2}{\bar{y}^2} \right] z(\bar{y}) = 0, \tag{54}$$

with solution

$$z(\bar{y}) = \bar{y}^{\beta'} Z_\nu \left(\mathrm{i} a \bar{y}^{\alpha'} \right),$$

where $Z_\nu(\bar{y}) = C_1 J_\nu(\bar{y}) + C_2 N_\nu(\bar{y})$ is the Bessel function. The boundary condition at infinity equals zero and due to the complex argument of the Bessel function (i is the imaginary unit), the solution is given by

$$z(\bar{y}) = \bar{y}^{\beta'} K_\nu \left(a \bar{y}^{\alpha'} \right),$$

where $K_\nu(\bar{y})$ is the modified Bessel function of the third kind. Here we find that

$$a = \frac{2}{2-\alpha} \sqrt{\frac{s+r}{\mathcal{D}_\alpha}}, \qquad \alpha' = \frac{2-\alpha}{2}, \qquad \beta' = \frac{2-3\alpha}{4}, \qquad \nu = \frac{1}{2}.$$

Thus, from the first equation in the system (53), we find the solution ($p = \frac{2}{2-\alpha}$)

$$\begin{aligned} \hat{P}_{r,\epsilon}(x,s|0) &= \mathcal{C}_\epsilon(s) \hat{f}(|x|,s|0) \\ &= \mathcal{C}_\epsilon(s) (\epsilon + |x|)^{\beta'} K_{1/2} \left(a(\epsilon + |x|)^{\alpha'} \right) \\ &= \mathcal{C}_\epsilon(s) (\epsilon + |x|)^{\beta' - \alpha'/2} \sqrt{\frac{\pi}{2a}} \mathrm{e}^{-a(\epsilon+|x|)^{\alpha'}}, \end{aligned} \tag{55}$$

where $a = p\sqrt{\frac{s+r}{\mathcal{D}_\alpha}}$, $\alpha' = \frac{1}{p}$, $\beta' = \frac{3-2p}{2p}$, while $\mathcal{C}_\epsilon(s)$ is obtained from the second equation in (53) and reads

$$\mathcal{C}_\epsilon(s) = \frac{\mathcal{D}_\alpha^{-3/4}}{\sqrt{2\pi/p}} s^{-1} (s+r)^{3/4} \exp\left(p \sqrt{\frac{s+r}{\mathcal{D}_\alpha}} \epsilon^{1/p} \right). \tag{56}$$

Therefore, the solution (55) becomes

$$\hat{P}_{r,\epsilon}(x,s|0) = \frac{s^{-1}(s+r)^{1/2}}{\sqrt{4\mathcal{D}_\alpha}} \left(\epsilon + |x| \right)^{-1+1/p} \exp\left(-p \sqrt{\frac{s+r}{\mathcal{D}_\alpha}} \left[\left(\epsilon + |x| \right)^{1/p} - \epsilon^{1/p} \right] \right). \tag{57}$$

In the limit $\epsilon \to 0$, we recover the result (19). In the absence of resetting the PDF becomes

$$\hat{P}_{0,\epsilon}(x,s|0) = \frac{s^{-1/2}}{\sqrt{4\mathcal{D}_\alpha}} \left(\epsilon + |x| \right)^{-1+1/p} \exp\left(-p \sqrt{\frac{s}{\mathcal{D}_\alpha}} \left[\left(\epsilon + |x| \right)^{1/p} - \epsilon^{1/p} \right] \right), \tag{58}$$

which by inverse Laplace transform yields

$$P_{0,\epsilon}(x,t) = \frac{\left(\epsilon + |x|\right)^{-1+1/p}}{\sqrt{4\pi \mathcal{D}_\alpha t}} \exp\left(-p^2 \frac{\left[\left(\epsilon + |x|\right)^{1/p} - \epsilon^{1/p}\right]^2}{4\mathcal{D}_\alpha t}\right). \tag{59}$$

From equation (57) one finds that the PDF in the presence of resetting can be derived from the PDF in the absence of resetting through the renewal equation

$$P_{r,\epsilon}(x,t|0) = \mathrm{e}^{-rt} P_{0,\epsilon}(x,t) + \int_0^t r\,\mathrm{e}^{-rt'} P_{0,\epsilon}(x,t')\mathrm{d}t'. \tag{60}$$

In the general case the integral has to be evaluated numerically.

4.2. MSD

From the PDF (57) we find the MSD

$$\begin{aligned}\left\langle x^2(s)\right\rangle_{r,\epsilon} = {} & \frac{2\mathcal{D}_\alpha^{p/2}}{p^{p-1}} \frac{s^{-1}}{(s+r)^{p/2}} \exp\left(p\sqrt{\frac{s+r}{\mathcal{D}_\alpha}}\epsilon^{1/p}\right) \\ & \times \left[\left(p\sqrt{\frac{s+r}{\mathcal{D}_\alpha}}\right)^{-p} \Gamma\left(2p, p\sqrt{\frac{s+r}{\mathcal{D}_\alpha}}\epsilon^{1/p}\right) - \epsilon\,\Gamma\left(p, p\sqrt{\frac{s+r}{\mathcal{D}_\alpha}}\epsilon^{1/p}\right)\right],\end{aligned} \tag{61}$$

where $\Gamma(a,z)$ is the incomplete gamma function. For $\epsilon \to 0$, we use that $\Gamma(a,z) \sim \Gamma(a)$ for $z \to 0$ and recover the result (32) for the MSD. In the long time limit, the MSD saturates,

$$\begin{aligned}\left\langle x^2(t)\right\rangle_{r,\epsilon} \sim \lim_{s\to 0} s\left\langle x^2(s)\right\rangle = {} & \frac{2}{p^{p-1}}\left(\frac{\mathcal{D}_\alpha}{r}\right)^{p/2} \exp\left(p\sqrt{\frac{r}{\mathcal{D}_\alpha}}\epsilon^{1/p}\right) \\ & \times \left[\frac{\Gamma\left(2p, p\sqrt{\frac{r}{\mathcal{D}_\alpha}}\epsilon^{1/p}\right)}{\left(p\sqrt{\frac{r}{\mathcal{D}_\alpha}}\right)^{p}} - \epsilon\,\Gamma\left(p, p\sqrt{\frac{r}{\mathcal{D}_\alpha}}\epsilon^{1/p}\right)\right].\end{aligned} \tag{62}$$

In the limit $\epsilon \to 0$, the MSD reduces to

$$\left\langle x^2(s)\right\rangle_{r,\epsilon=0} = \frac{2\mathcal{D}_\alpha^{p/2}}{p^{p-1}} \frac{s^{-1}}{(s+r)^{p/2}} \left(p\sqrt{\frac{s+r}{\mathcal{D}_\alpha}}\right)^{-p} \Gamma(2p) = \frac{\Gamma(2p+1)}{p^{2p}} \mathcal{D}_\alpha^p \frac{s^{-1}}{(s+r)^p}, \tag{63}$$

which by inverse Laplace transform becomes

$$\left\langle x^2(t)\right\rangle_{r,\epsilon=0} = \frac{\Gamma(1+2p)}{p^{2p}} \mathcal{D}_\alpha^p t^p E_{1,p+1}^p(-rt) = \frac{\Gamma(1+2p)}{p^{2p}} \frac{\mathcal{D}_\alpha^p}{r^p}\left[1 - \frac{\Gamma(p,rt)}{\Gamma(p)}\right], \tag{64}$$

and is equivalent to the result (32).

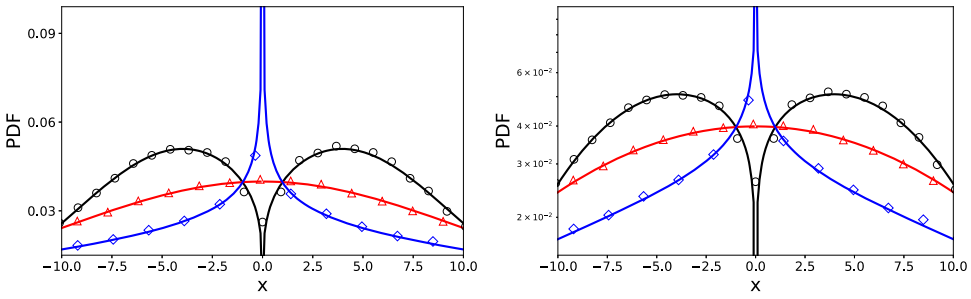

Figure 8. PDF (59) in absence of resetting for $\mathcal{D}_\alpha = 1$, $x_0 = 0$, $t = 50$, $r = 0$ and $\alpha = 0.5$ (blue line: exact solution; squares: simulations), $\alpha = 0$ (red line: exact solution; triangles: simulations), $\alpha = -0.5$ (black line: exact solution; circles: simulations). The PDF is shown using linear scale in the left panel and in for log–linear scale in the right panel.

4.3. NESS and LDF

From the PDF (57) in Laplace space, we find that in the long time limit the solution reaches a NESS, given by

$$P_{\rm st}(x) = \lim_{s\to 0} sP_{r,\epsilon}(x,s|0) = \frac{r^{1/2}}{\sqrt{4\mathcal{D}_\alpha}}\left(\epsilon+|x|\right)^{-1+1/p}\exp\left(-p\sqrt{\frac{r}{\mathcal{D}_\alpha}}\left[\left(\epsilon+|x|\right)^{1/p}-\epsilon^{1/p}\right]\right). \tag{65}$$

The way to calculate the LDF is the same as in section 3.3. Following the procedure outlined there, we find

$$\Phi(\tau,w) = r\tau + \frac{p^2}{4\mathcal{D}\tau}w^2, \tag{66}$$

where

$$w = \frac{(\epsilon+|x|)^{1/p}-\epsilon^{1/p}}{t}.$$

For the extremum point we then obtain $\tau_* = \frac{p}{\sqrt{4\mathcal{D}_\alpha r}}w$, and the LDF becomes

$$I(w) = \begin{cases} p\sqrt{\dfrac{r}{\mathcal{D}}}\,\dfrac{(\epsilon+|x|)^{1/p}-\epsilon^{1/p}}{t}, & (\epsilon+|x|)^{1/p} \leqslant \epsilon^{1/p} + \dfrac{(4\mathcal{D}_\alpha r)^{1/2}}{p}\,t, \\ r + \dfrac{p^2}{4\mathcal{D}_\alpha}\left(\dfrac{(\epsilon+|x|)^{1/p}-\epsilon^{1/p}}{t}\right)^2, & (\epsilon+|x|)^{1/p} \geqslant \epsilon^{1/p} + \dfrac{(4\mathcal{D}_\alpha r)^{1/2}}{p}\,t. \end{cases} \tag{67}$$

4.4. Numerical simulations

We again consider the Langevin equation (48) in the presence of resetting, based on the regularised diffusion coefficient $\mathcal{D}(x) = \mathcal{D}_\alpha(\epsilon+|x|)^\alpha$ and the same parameters as in section 3.4. The initial position of the particle is at the origin, $x_0 = 0$. A comparison between the analytical

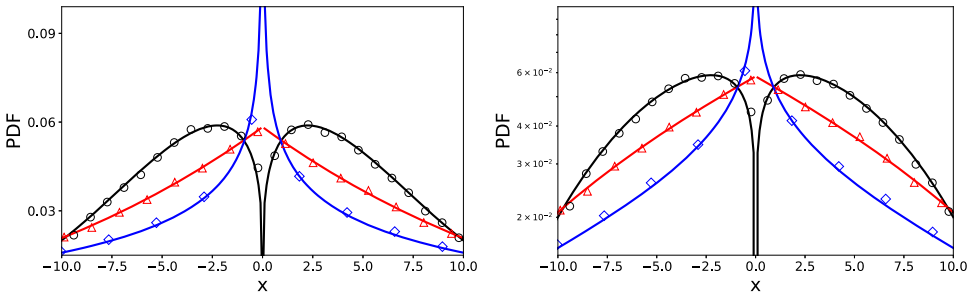

Figure 9. PDF (60) in case of resetting for $\mathcal{D}_\alpha = 1$, $x_0 = 0$, $t = 50$, $r = 0.01$ and $\alpha = 0.5$ (blue line: exact solution; squares: simulations), $\alpha = 0$ (red line: exact solution; triangles: simulations), $\alpha = -0.5$ (black line: exact solution; circles: simulations). The PDF is shown using linear scale in the left panel and for log–linear scale in the right panel.

results for the PDF, obtained via the numerical inverse Laplace transform algorithm in Mathematica [70] and the simulations results for different values of the parameter α are shown in figures 8 and 9 in the absence and presence of resetting, respectively. Very good agreement is observed.

5. Summary

We presented a detailed analysis of an HDP in the presence of stochastic resetting with Poissonian statistic. The heterogeneity is characterised by the position-dependent diffusion coefficient $\mathcal{D}(x) \sim |x|^\alpha$, $\alpha < 2$, and using the Stratonovich interpretation of the Langevin equation of motion. In the short time limit compared to the inverse resetting rate, we reproduce all results for the PDF and MSD for the case without resetting. In the long time limit, we show how the MSD saturates due to the resetting mechanism, and how the corresponding PDF reaches a NESS. The transition to this state is analysed in terms of the LDF. We showed that the diffusion length in the presence of resetting scales like $\xi \simeq t^p$, in contrast to the scaling $\xi \simeq t^{p/2}$ in the absence of resetting. In particular, we show that the boundary separating the central region, in which the NESS is achieved, from the domain, in which the system is still in a transient state, expands with the non-constant velocity $v(t) \simeq t^{\alpha/(2-\alpha)}$. In the normal diffusion case ($\alpha = 0$) this result corresponds to the known formula with a constant velocity of the boundary movement. The analytical results were verified by extensive numerical simulations using the Langevin equation with resetting. Similar analysis can be performed for the Itô and Hänggi–Klimontovich interpretation of the HDP, and we leave it as a task for future research. Our further research includes the study of the first passage properties of HDP with resetting as well as similar analysis of the other prescriptions (Itô and Hänggi–Klimontovich) and differences/similarities between them. We also note that very recently the first study of heterogeneous process with resetting in Hänggi–Klimontovich interpretation was undertaken in reference [76].

Acknowledgments

TS was supported by the Alexander von Humboldt Foundation. RM acknowledges support from the Foundation for Polish Science (Fundacja na rzecz Nauki Polskiej, FNR) within an

Alexander von Humboldt Honorary Polish Research Scholarship. AC acknowledges support of the Polish National Agency for Academic Exchange (NAWA). TS, VD and LK also acknowledge support from the bilateral Macedonian-Chinese research project 20-6333, funded under the intergovernmental Macedonian-Chinese agreement. The authors acknowledge financial support by the German Science Foundation (DFG, Grant No. ME 1535/12-1).

Data availability statement

All data that support the findings of this study are included within the article (and any supplementary files).

Appendix A. Calculation of moments

Here we provide a detailed calculation of the moments $\langle x^n(t)\rangle = \int_{-\infty}^{\infty} x^n P(x,t)\mathrm{d}x$, where $n = 0, 1, 2, \ldots$, of the PDF (18). For even moments $n = 2m$, with $m = 0, 1, 2, \ldots$, we have

$$\begin{aligned}\langle x^{2m}(t)\rangle &= \int_{-\infty}^{\infty} \frac{x^{2m}|x|^{1/p-1}}{\sqrt{4\pi\mathcal{D}_\alpha t}} \exp\left(-\frac{p^2\left[\mathrm{sgn}(x)\,|x|^{1/p} - \mathrm{sgn}(x_0)\,|x_0|^{1/p}\right]^2}{4\mathcal{D}_\alpha t}\right)\mathrm{d}x \\ &= \int_0^{\infty} \frac{x^{2m}x^{1/p-1}}{\sqrt{4\pi\mathcal{D}_\alpha t}} \exp\left(-\frac{p^2\left[x^{1/p} - \mathrm{sgn}(x_0)\,|x_0|^{1/p}\right]^2}{4\mathcal{D}_\alpha t}\right)\mathrm{d}x \\ &\quad + \int_{-\infty}^{0} \frac{x^{2m}|x|^{1/p-1}}{\sqrt{4\pi\mathcal{D}_\alpha t}} \exp\left(-\frac{p^2\left[|x|^{1/p} + \mathrm{sgn}(x_0)\,|x_0|^{1/p}\right]^2}{4\mathcal{D}_\alpha t}\right)\mathrm{d}x \\ &= I_{\mathrm{e},1} + I_{\mathrm{e},2}. \end{aligned} \tag{A.1}$$

For the first integral, by introducing $x^{1/p} = y$, i.e. $\frac{1}{p}x^{1/p-1}\,\mathrm{d}x = \mathrm{d}y$, we find

$$I_{\mathrm{e},1} = \int_0^{\infty} \frac{p\,y^{2mp}}{\sqrt{4\pi\mathcal{D}_\alpha t}} \exp\left(-\frac{p^2\left[y - \mathrm{sgn}(x_0)\,|x_0|^{1/p}\right]^2}{4\mathcal{D}_\alpha t}\right)\mathrm{d}y, \tag{A.2}$$

while for the second integral, where we first introduce $z = -x$ and then $z^{1/p} = y$, we find

$$I_{\mathrm{e},2} = \int_0^{\infty} \frac{p\,y^{2mp}}{\sqrt{4\pi\mathcal{D}_\alpha t}} \exp\left(-\frac{p^2\left[y + \mathrm{sgn}(x_0)\,|x_0|^{1/p}\right]^2}{4\mathcal{D}_\alpha t}\right)\mathrm{d}y. \tag{A.3}$$

Thus, for the even moments, we have

$$\begin{aligned}\langle x^{2m}(t)\rangle &= \frac{2p\exp\left(-\frac{p^2}{4\mathcal{D}_\alpha t}|x_0|^{2/p}\right)}{\sqrt{4\pi\mathcal{D}_\alpha t}} \int_0^{\infty} y^{2mp}\exp\left(-\frac{p^2}{4\mathcal{D}_\alpha t}y^2\right)\cosh\left(2\,\mathrm{sgn}(x_0)\,|x_0|^{1/p}y\right)\mathrm{d}y \\ &= \frac{2p\exp\left(-\frac{p^2}{4\mathcal{D}_\alpha t}|x_0|^{2/p}\right)}{\sqrt{4\pi\mathcal{D}_\alpha t}} \frac{\Gamma(2mp+1)}{2\left(2\frac{p^2}{4\mathcal{D}_\alpha t}\right)^{mp+1/2}} \exp\left(\frac{1}{2}\frac{p^2}{4\mathcal{D}_\alpha t}|x_0|^{2/p}\right) \\ &\quad \times \left[D_{-(2mp+1)}\left(-\sqrt{2\frac{p^2}{4\mathcal{D}_\alpha t}}|x_0|^{1/p}\right) + D_{-(2mp+1)}\left(\sqrt{2\frac{p^2}{4\mathcal{D}_\alpha t}}|x_0|^{1/p}\right)\right], \end{aligned} \tag{A.4}$$

where $D_\mu(z)$ are parabolic cylinder functions [75], given by

$$D_\mu(z) = 2^{\mu/2}\,\mathrm{e}^{-\frac{z^2}{4}}\left[\frac{\sqrt{\pi}}{\Gamma\left(\frac{1-\mu}{2}\right)}{}_1F_1\left(-\frac{\mu}{2},\frac{1}{2},\frac{z^2}{2}\right)-\frac{\sqrt{2\pi}z}{\Gamma\left(-\frac{\mu}{2}\right)}{}_1F_1\left(\frac{1-\mu}{2},\frac{3}{2},\frac{z^2}{2}\right)\right]. \tag{A.5}$$

This yields

$$\langle x^{2m}(t)\rangle = \frac{\Gamma(mp+1/2)}{p^{2mp}\sqrt{\pi}}(4\mathcal{D}_\alpha t)^{mp}{}_1F_1\left(-mp,\frac{1}{2},-\frac{p^2}{4\mathcal{D}_\alpha t}|x_0|^{2/p}\right), \tag{A.6}$$

where we use the property

$${}_1F_1(a,b,z) = \mathrm{e}^z{}_1F_1(b-a,b,-z). \tag{A.7}$$

From here we find that $\langle x^0(t)\rangle = 1$, i.e. the PDF is normalised, while for the MSD and fourth moment, we obtain

$$\langle x^2(t)\rangle = \frac{\Gamma(p+1/2)}{p^{2p}\sqrt{\pi}}(4\mathcal{D}_\alpha t)^{p}{}_1F_1\left(-p,\frac{1}{2},-\frac{p^2}{4\mathcal{D}_\alpha t}|x_0|^{2/p}\right) \tag{A.8}$$

and

$$\langle x^4(t)\rangle = \frac{\Gamma(2p+1/2)}{p^{4p}\sqrt{\pi}}(4\mathcal{D}_\alpha t)^{2p}{}_1F_1\left(-2p,\frac{1}{2},-\frac{p^2}{4\mathcal{D}_\alpha t}|x_0|^{2/p}\right), \tag{A.9}$$

respectively. By using $\Gamma(z)\Gamma(z+1/2) = 2^{1-2z}\sqrt{\pi}\,\Gamma(2z)$ with $z = p+1/2$ in equation (A.8), we obtain equation (20).

For odd moments $n = 2m+1$, with $m = 0,1,2,\ldots$, we have

$$\begin{aligned}\langle x^{2m+1}(t)\rangle &= \int_{-\infty}^{\infty}\frac{x^{2m+1}|x|^{1/p-1}}{\sqrt{4\pi\mathcal{D}_\alpha t}}\exp\left(-\frac{p^2\left[\mathrm{sgn}(x)\,|x|^{1/p}-\mathrm{sgn}(x_0)\,|x_0|^{1/p}\right]^2}{4\mathcal{D}_\alpha t}\right)\mathrm{d}x\\ &= \int_0^{\infty}\frac{x^{2m+1}x^{1/p-1}}{\sqrt{4\pi\mathcal{D}_\alpha t}}\exp\left(-\frac{p^2\left[x^{1/p}-\mathrm{sgn}(x_0)\,|x_0|^{1/p}\right]^2}{4\mathcal{D}_\alpha t}\right)\mathrm{d}x\\ &\quad+\int_{-\infty}^{0}\frac{x^{2m+1}|x|^{1/p-1}}{\sqrt{4\pi\mathcal{D}_\alpha t}}\exp\left(-\frac{p^2\left[|x|^{1/p}+\mathrm{sgn}(x_0)\,|x_0|^{1/p}\right]^2}{4\mathcal{D}_\alpha t}\right)\mathrm{d}x\\ &= I_{\mathrm{o},1}+I_{\mathrm{o},2}.\end{aligned} \tag{A.10}$$

In the first integral we introduce $x^{1/p} = y$, to find

$$I_{\mathrm{o},1} = \int_0^{\infty}\frac{p\,y^{(2m+1)p}}{\sqrt{4\pi\mathcal{D}_\alpha t}}\exp\left(-\frac{p^2\left[y-\mathrm{sgn}(x_0)\,|x_0|^{1/p}\right]^2}{4\mathcal{D}_\alpha t}\right)\mathrm{d}y, \tag{A.11}$$

while in the second integral we first introduce $z=-x$ and then $z^{1/p}=y$ to find

$$I_{\mathrm{o},2}=-\int_0^\infty \frac{p\,y^{(2m+1)p}}{\sqrt{4\pi\mathcal{D}_\alpha t}}\exp\left(-\frac{p^2\left[y+\mathrm{sgn}(x_0)\,|x_0|^{1/p}\right]^2}{4\mathcal{D}_\alpha t}\right)\mathrm{d}y. \tag{A.12}$$

The odd moments become

$$\begin{aligned}\langle x^{2m+1}(t)\rangle &= \frac{2p\,\exp\left(-\frac{p^2}{4\mathcal{D}_\alpha t}|x_0|^{2/p}\right)}{\sqrt{4\pi\mathcal{D}_\alpha t}}\\ &\quad\times\int_0^\infty y^{(2m+1)p}\,\exp\left(-\frac{p^2}{4\mathcal{D}_\alpha t}y^2\right)\sinh\left(2\,\mathrm{sgn}(x_0)\,|x_0|^{1/p}y\right)\mathrm{d}y\\ &= \frac{2p\,\exp\left(-\frac{p^2}{4\mathcal{D}_\alpha t}|x_0|^{2/p}\right)}{\sqrt{4\pi\mathcal{D}_\alpha t}}\,\frac{\Gamma([2m+1]p+1)}{2\left(2\frac{p^2}{4\mathcal{D}_\alpha t}\right)^{mp+(p+1)/2}}\exp\left(\frac{1}{2}\frac{p^2}{4\mathcal{D}_\alpha t}|x_0|^{2/p}\right)\\ &\quad\times\left[D_{-([2m+1]p+1)}\left(-\sqrt{2\frac{p^2}{4\mathcal{D}_\alpha t}}\,\mathrm{sgn}(x_0)|x_0|^{1/p}\right)\right.\\ &\quad\left.-\,D_{-([2mp+1]+1)}\left(\sqrt{2\frac{p^2}{4\mathcal{D}_\alpha t}}\,\mathrm{sgn}(x_0)|x_0|^{1/p}\right)\right],\end{aligned} \tag{A.13}$$

which can be transformed to

$$\begin{aligned}\langle x^{2m+1}(t)\rangle &= \frac{2p\Gamma\left(\frac{[2m+1]p}{2}+1\right)}{p^{(2m+1)p}\sqrt{\pi}}(4\mathcal{D}_\alpha t)^{\frac{(2m+1)p-1}{2}}\,\mathrm{sgn}(x_0)|x_0|^{1/p}\\ &\quad\times{}_1F_1\left(\frac{1-(2m+1)p}{2},\frac{3}{2},-\frac{p^2}{4\mathcal{D}_\alpha t}|x_0|^{2/p}\right).\end{aligned} \tag{A.14}$$

Therefore, the first and third moments read

$$\langle x(t)\rangle=\frac{2p\Gamma\left(\frac{p}{2}+1\right)}{p^p\sqrt{\pi}}(4\mathcal{D}_\alpha t)^{\frac{p-1}{2}}\,\mathrm{sgn}(x_0)|x_0|^{1/p}{}_1F_1\left(\frac{1-p}{2},\frac{3}{2},-\frac{p^2}{4\mathcal{D}_\alpha t}|x_0|^{2/p}\right) \tag{A.15}$$

and

$$\langle x^3(t)\rangle=\frac{2p\Gamma\left(\frac{3p}{2}+1\right)}{p^{3p}\sqrt{\pi}}(4\mathcal{D}_\alpha t)^{\frac{3p-1}{2}}\,\mathrm{sgn}(x_0)|x_0|^{1/p}{}_1F_1\left(\frac{1-3p}{2},\frac{3}{2},-\frac{p^2}{4\mathcal{D}_\alpha t}|x_0|^{2/p}\right), \tag{A.16}$$

respectively. Knowing the first fourth moments one can calculate the kurtosis and skewness of the PDF.

Appendix B. Equivalent formulations of HDP with stochastic resetting

Here we provide alternative approaches to the HDP. Let us consider the Fokker–Planck equation for the PDF $P_r(x,t|x_0)$,

$$\frac{\partial}{\partial t}P_r(x,t|x_0) = \frac{\partial}{\partial x}\left\{\sqrt{\mathcal{D}(x)}\frac{\partial}{\partial x}\left[\sqrt{\mathcal{D}(x)}P_r(x,t|x_0)\right]\right\} - rP_r(x,t|x_0) + r\delta(x-x_0), \tag{B.1}$$

with initial position $P_r(x,t=0|x_0)=\delta(x-x_0)$, where r is the rate of resetting to this initial position x_0. The second term on the right-hand side of equation (B.1) represents the loss of probability from position x due to reset to x_0, and the third term accounts for the gain of probability at x_0 due to resetting from all other positions. For $\alpha=0$ one obtains the standard diffusion equation with stochastic resetting [26, 27, 41].

By using the Laplace transform of equation (B.1) we have

$$\begin{aligned} s\hat{P}_r(x,s|x_0) - \delta(x-x_0) = {} & \frac{\partial}{\partial x}\left\{\sqrt{\mathcal{D}(x)}\frac{\partial}{\partial x}\left[\sqrt{\mathcal{D}(x)}P_r(x,s|x_0)\right]\right\} \\ & - r\hat{P}_r(x,s|x_0) + \frac{r}{s}\delta(x-x_0), \end{aligned} \tag{B.2}$$

which can be rewritten as

$$s\hat{P}_r(x,s|x_0) - \delta(x-x_0) = s\times\frac{1}{s+r}\frac{\partial}{\partial x}\left\{\sqrt{\mathcal{D}(x)}\frac{\partial}{\partial x}\left[\sqrt{\mathcal{D}(x)}\hat{P}_r(x,s|x_0)\right]\right\}. \tag{B.3}$$

The inverse Laplace transform yields the heterogeneous diffusion equation with exponential memory kernel,

$$\frac{\partial}{\partial t}P_r(x,t|x_0) = \frac{\partial}{\partial t}\int_0^t \eta(t-t')\frac{\partial}{\partial x}\left\{\sqrt{\mathcal{D}(x)}\frac{\partial}{\partial x}\left[\sqrt{\mathcal{D}(x)}P_r(x,t'|x_0)\right]\right\}\mathrm{d}t', \tag{B.4}$$

where $\eta(t)=\mathrm{e}^{-rt}$, which is equivalent to equation (B.1), see also [77]. This is the second possible form of HDP with resetting. We note that the HDP with memory kernel from the left-hand side of the equation, for $x_0=0$ has been recently analysed in reference [78].

Let us now consider the heterogeneous diffusion equation (5) without resetting. By applying the Laplace transform we have

$$s\hat{P}(x,s) - \delta(x-x_0) = \frac{\partial}{\partial x}\left\{\sqrt{\mathcal{D}(x)}\frac{\partial}{\partial x}\left[\sqrt{\mathcal{D}(x)}P(x,s)\right]\right\}. \tag{B.5}$$

By using $s\to s+r$ it becomes

$$(s+r)\hat{P}(x,s+r) - \delta(x-x_0) = \frac{\partial}{\partial x}\left\{\sqrt{\mathcal{D}(x)}\frac{\partial}{\partial x}\left[\sqrt{\mathcal{D}(x)}P(x,s+r)\right]\right\}, \tag{B.6}$$

i.e.

$$\frac{s+r}{s}\hat{P}(x,s+r) - \frac{1}{s}\delta(x-x_0) = \frac{1}{s+r}\frac{\partial}{\partial x}\left\{\sqrt{\mathcal{D}(x)}\frac{\partial}{\partial x}\left[\sqrt{\mathcal{D}(x)}\frac{s+r}{s}P(x,s+r)\right]\right\}. \tag{B.7}$$

Let us introduce the function $P_r(x,t|x_0)$, which in Laplace space is defined by

$$\hat{P}_r(x,s|x_0) = \frac{s+r}{s}\hat{P}(x,s+r). \tag{B.8}$$

From this equation we notice that the PDF in the presence of resetting can be represented by

$$\hat{P}_r(x,s|x_0) = \frac{s+r}{s}\hat{P}(x,s+r) = \frac{s+r}{s}\int_0^\infty P(x,u)\mathrm{e}^{-u(s+r)}\,\mathrm{d}u, \tag{B.9}$$

which has the form of a subordination integral in Laplace space,

$$\hat{P}_r(x,s|x_0) = \int_0^\infty P(x,u)\hat{h}(u,s)\mathrm{d}u, \tag{B.10}$$

where

$$\hat{h}(u,s) = \frac{s+r}{s}\mathrm{e}^{-u(s+r)} \tag{B.11}$$

is the so-called subordination function (for details on subordination see [6, 79]). By inverse Laplace transform of equation (B.10) we arrive at the known form for the subordination integral,

$$P_r(x,t|x_0) = \int_0^\infty P(x,u)h(u,t)\mathrm{d}u, \tag{B.12}$$

where

$$h(u,t) = \mathscr{L}^{-1}\left[\frac{s+r}{s}\mathrm{e}^{-u(s+r)}\right] = \mathrm{e}^{-rt}\,\delta(t-u) + r\,\mathrm{e}^{-ru}\,\theta(t-u).$$

Therefore,

$$\begin{aligned} P_r(x,t|x_0) &= \int_0^\infty \left[\mathrm{e}^{-rt}\,\delta(t-u) + r\,\mathrm{e}^{-ru}\theta(t-u)\right]P(x,u)\mathrm{d}u \\ &= \mathrm{e}^{-rt}P(x,t) + \int_0^t r\,\mathrm{e}^{-ru}P(x,u)\mathrm{d}u, \end{aligned} \tag{B.13}$$

which is the renewal equation (23). This is the third possible representation of the HDP with resetting, in addition to those in equations (B.1) and (B.4).

ORCID iDs

Trifce Sandev https://orcid.org/0000-0001-9120-3847
Ralf Metzler https://orcid.org/0000-0002-6013-7020

References

[1] Bouchaud J-P and Georges A 1990 *Phys. Rep.* **195** 127
[2] Höfling F and Franosch T 2013 *Rep. Prog. Phys.* **76** 046602
[3] Barkai E, Garini Y and Metzler R 2012 *Phys. Today* **65** 29
[4] Sokolov I M 2012 *Soft Matter* **8** 9043

[5] Krapf D and Metzler R 2019 *Phys. Today* **72** 48
[6] Metzler R and Klafter J 2000 *Phys. Rep.* **339** 1
Metzler R and Klafter J 2004 *J. Phys. A: Math. Gen.* **37** R161
[7] Kolmogorov A N 1940 *C. R. (Dokl.) Acad. Sci. URSS* **26** 115
Mandelbrot B B and Van Ness J W 1968 *SIAM Rev.* **10** 422
[8] Goychuk I 2012 *Adv. Chem. Phys.* **150** 187
[9] English B P, Hauryliuk V, Sanamrad A, Tankov S, Dekker N H and Elf J 2011 *Proc. Natl Acad. Sci.* **108** E365
[10] Kühn T, Ihalainen T O, Hyväluoma J, Dross N, Willman S F, Langowski J, Vihinen-Ranta M and Timonen J 2011 *PLoS One* **6** e22962
[11] Platani M, Goldberg I, Lamond A I and Swedlow J R 2002 *Nat. Cell Biol.* **4** 502
[12] Haggerty R and Gorelick S M 1995 *Water Resour. Res.* **31** 2383
[13] Dentz M, Gouze P, Russian A, Dweik J and Delay F 2012 *Adv. Water Resour.* **49** 13
[14] Cherstvy A G, Chechkin A V and Metzler R 2013 *New J. Phys.* **15** 083039
[15] Loverdo C, Bénichou O, Voituriez R, Biebricher A, Bonnet I and Desbiolles P 2009 *Phys. Rev. Lett.* **102** 188101
[16] O'Shaughnessy B and Procaccia I 1985 *Phys. Rev. Lett.* **54** 455
[17] Regev S, Gronhech-Jensen N and Farago O 2016 *Phys. Rev.* E **94** 012116
Regev S 2017 Diffusion in inhomogeneous systems *Doctoral Dissertation* Ben-Gurion University of the Negev
[18] Cherstvy A G and Metzler R 2013 *Phys. Chem. Chem. Phys.* **15** 20220
Cherstvy A G, Chechkin A V and Metzler R 2014 *Soft Matter* **10** 1591
Cherstvy A G and Metzler R 2014 *Phys. Rev.* E **90** 012134
[19] Srokowski T 2007 *Phys. Rev.* E **75** 051105
Srokowski T 2009 *Phys. Rev.* E **80** 051113
Srokowski T 2014 *Phys. Rev.* E **89** 030102
Srokowski T 2009 *Phys. Rev.* E **79** 040104
Srokowski T 2017 *Phys. Rev.* E **95** 032133
Srokowski T and Kamińska A 2006 *Phys. Rev.* E **74** 021103
Srokowski T and Kamińska A 2017 *Phys. Rev.* E **96** 032105
[20] Kazakevicius R and Ruseckas J 2016 *Phys. Rev.* E **94** 032109
[21] Fa K S and Lenzi E K 2003 *Phys. Rev.* E **67** 061105
Fa K S 2005 *Phys. Rev.* E **72** 020101
De Andrade M F, Lenzi E K, Evangelista L R, Mendes R S and Malacarne L C 2005 *Phys. Lett.* A **347** 160
Silva A T, Lenzi E K, Evangelista L R, Lenzi M K, Ribeiro H V and Tateishi A A 2011 *J. Math. Phys.* **52** 083301
Fa K S 2011 *Phys. Rev.* E **84** 012102
Fa K S 1989 *Ann. Phys.* **501** 327
[22] Lau A W C and Lubensky T C 2007 *Phys. Rev.* E **76** 011123
Fulinski A 2011 *Phys. Rev.* E **83** 061140
[23] Sandev T, Iomin A and Kocarev L 2020 *Phys. Rev.* E **102** 042109
[24] Leibovich N and Barkai E 2019 *Phys. Rev.* E **99** 042138
[25] Dos Santos M A F, Dornelas V, Colombo E H and Anteneodo C 2020 *Phys. Rev.* E **102** 042139
[26] Evans M R and Majumdar S N 2011 *Phys. Rev. Lett.* **106** 160601
[27] Evans M R and Majumdar S N 2011 *J. Phys. A: Math. Theor.* **44** 435001
[28] Evans M R, Majumdar S N and Schehr G 2020 *J. Phys. A: Math. Theor.* **53** 193001
[29] Méndez V and Campos D 2016 *Phys. Rev.* E **93** 022106
[30] Redner S 2007 *A Guide to First-Passage Processes* (Cambridge: Cambridge University Press)
[31] Pal A, Eliazar I and Reuveni S 2019 *Phys. Rev. Lett.* **122** 020602
[32] Reuveni S 2016 *Phys. Rev. Lett.* **116** 170601
[33] Pal A and Reuveni S 2017 *Phys. Rev. Lett.* **118** 030603
[34] Ahmad S, Nayak I, Bansal A, Nandi A and Das D 2019 *Phys. Rev.* E **99** 022130
[35] Kusmierz L, Majumdar S N, Sabhapandit S and Schehr G 2014 *Phys. Rev. Lett.* **113** 220602
[36] Chechkin A and Sokolov I M 2018 *Phys. Rev. Lett.* **121** 050601
[37] Campos D and Méndez V 2015 *Phys. Rev.* E **92** 062115
Méndez V, Masó-Puigdellosas A, Sandev T and Campos D 2021 *Phys. Rev.* E **103** 022103
[38] Dahlenburg M, Chechkin A V, Schumer R and Metzler R 2021 *Phys. Rev.* E **103** 052123

[39] Pal A, Kusmierz L and Reuveni S 2020 *Phys. Rev. Res.* **2** 043174
[40] Ray S, Mondal D and Reuveni S 2019 *J. Phys. A: Math. Theor.* **52** 255002
[41] Pal A, Kundu A and Evans M R 2016 *J. Phys. A: Math. Theor.* **49** 225001
Gupta D, Pal A and Kundu A 2021 *J. Stat. Mech.* 043202
[42] Bodrova A S and Sokolov I M 2020 *Phys. Rev.* E **101** 052130
Bodrova A S and Sokolov I M 2020 *Phys. Rev.* E **101** 062117
[43] Kusmierz L and Gudowska-Nowak E 2019 *Phys. Rev.* E **99** 052116
Capala K, Dybiec B and Gudowska-Nowak E 2021 *Chaos* **31** 063123
[44] Mukherjee B, Sengupta K and Majumdar S N 2018 *Phys. Rev.* B **98** 104309
[45] Rose D C, Touchette H, Lesanovsky I and Garrahan J P 2018 *Phys. Rev.* E **98** 022129
[46] Stojkoski V, Sandev T, Kocarev L and Pal A 2021 *Phys. Rev.* E **104** 014121
[47] Wang W, Cherstvy A, Kantz H, Metzler R and Sokolov I 2021 *Phys. Rev.* E **104** 024105
[48] Tal-Friedman O, Pal A, Sekhon A, Reuveni S and Roichman Y 2021 *J. Phys. Chem. Lett.* **11** 7350
[49] Itô K 1944 *Proc. of the Imperial Academy* vol 20 p 519
[50] Gikhman I I and Skorokhod A V 1979 *The Theory of Stochastic Processes III* (Berlin: Springer)
[51] Stratonovich R L 1966 *SIAM J. Control* **4** 362
Stratonovich R 1964 *Vestn. Mosk. Univ.* **1** 2 (in Russian)
[52] Hänggi P 1978 *Helv. Phys. Acta* **51** 183
Hänggi P 1980 *Helv. Phys. Acta* **53** 491
Dunkel J and Hänggi P 2005 *Phys. Rev.* E **72** 036106
[53] Klimontovich Y L 1990 *Physica* A **163** 515
Klimontovich Y L 1994 *Phys.-Usp.* **37** 737
[54] Van Kampen N G 1981 *J. Stat. Phys.* **24** 175
[55] Sancho J M and García-Ojalvo J 2000 Noise-induced order in extended systems: a tutorial *Stochastic Processes in Physics, Chemistry, and Biology* (*Lecture Notes in Physics* vol 557) ed Freund J A and Poeschel T (Berlin: Springer) pp 235–46
Carrillo O, Ibañes M, Garcáa-Ojalvo J, Casademunt J and Sancho J M 2003 *Phys. Rev.* E **67** 046110
[56] West B J, Bulsara A R, Lindenberg K, Seshadri V and Shuler K E 1979 *Physica* A **97** 211
Bulsara A R, Lindenberg K, Seshadri V, Shuler K E and West B J 1979 *Physica* A **97** 234
[57] Fang X, Kruse K, Lu T and Wang J 2019 *Rev. Mod. Phys.* **91** 045004
Ritort F 2007 *Adv. Chem. Phys.* **137** 31
[58] Wang W, Seno F, Sokolov I M, Chechkin A V and Metzler R 2020 *New J. Phys.* **22** 083041
[59] Domazetoski V, Chechkin A, Kocarev L, Metzler R, and Sandev T in preparation
[60] Stojkoski V, Sandev T, Basnarkov L, Kocarev L and Metzler R 2020 *Entropy* **22** 1432
[61] Dos Santos M A F and Menon Junior L 2020 *Physics* **2** 571
[62] Evans M R and Majumdar S N 2014 *J. Phys. A: Math. Theor.* **47** 285001
[63] Bodrova A S, Chechkin A V and Sokolov I M 2019 *Phys. Rev.* E **100** 012120
Bodrova A S, Chechkin A V and Sokolov I M 2019 *Phys. Rev.* E **100** 012119
[64] Masó-Puigdellosas A, Campos D and Méndez V 2019 *Phys. Rev.* E **100** 042104
[65] Prabhakar T R 1971 *Yokohama Math. J.* **19** 7
[66] Garra R and Garrappa R 2018 *Commun. Nonlinear Sci. Numer. Simul.* **56** 314
Sandev T, Chechkin A V, Korabel N, Kantz H, Sokolov I M and Metzler R 2015 *Phys. Rev.* E **92** 042117
Giusti A, Colombaro I, Garra R, Garrappa R, Polito F, Popolizio M and Mainardi F 2020 *Fract. Calc. Appl. Anal.* **23** 9
Bazhlekova E 2021 *Fract. Calc. Appl. Anal.* **24** 88
[67] Majumdar S N, Sabhapandit S and Schehr G 2015 *Phys. Rev.* E **91** 052131
[68] Singh R K, Metzler R and Sandev T 2020 *J. Phys. A: Math. Theor.* **53** 505003
Singh R K, Sandev T, Iomin A and Metzler R 2021 *J. Phys. A: Math. Theor.* **54** 404006
[69] Arfken G B and Weber H J 2005 *Mathematical Methods for Physicists* 6th edn (Amsterdam: Elsevier)
[70] Mallet A 2000 *Numerical Inversion of Laplace Transform* (Wolfram Library Archive) pp 210–968
[71] Pal A 2015 *Phys. Rev.* E **91** 012113
[72] Sandev T, Domazetoski V, Iomin A and Kocarev L 2021 *Mathematics* **9** 221
Domazetoski V, Masó-Puigdellosas A, Sandev T, Méndez V, Iomin A and Kocarev L 2020 *Phys. Rev. Res.* **2** 033027
[73] Sandev T, Schulz A, Kantz H and Iomin A 2018 *Chaos Solitons Fractals* **114** 551
[74] Li Y, Mei R, Xu Y, Kurths J, Duan J and Metzler R 2020 *New J. Phys.* **22** 053016

[75] Gradshteyn I S and Ryzhik I M 2007 *Table of Integrals, Series, and Products* (Academic)
[76] Lenzi M K, Lenzi E K, Guilherme L M S, Evangelista L R and Ribeiro H V 2021 *Physica* A **588** 126560
[77] Tateishi A A, Ribeiro H V and Lenzi E K 2017 *Front. Phys.* **5** 52
Tateishi A A, Ribeiro H V, Sandev T, Petreska I and Lenzi E K 2020 *Phys. Rev.* E **101** 022135
[78] Fa K S 2021 *Phys. Scr.* **96** 055002
dos Santos M A F and Gomez I S 2018 *J. Stat. Mech.* 123205
[79] Baule A and Friedrich R 2005 *Phys. Rev.* E **71** 026101
Chechkin A V, Hofmann M and Sokolov I M 2009 *Phys. Rev.* E **80** 031112
Sandev T, Metzler R and Chechkin A 2018 *Fract. Calc. Appl. Anal.* **21** 10